Simulation Study of Quadrupole Dielectrophoretic Trapping

W.H. Li, J. Sun, B. Liu, and X. Z. Zhang
School of Mechanical, Materials and Mechatronic Engineering, University of Wollongong,
Northfields Avenue, NSW 2522, Australia

Abstract: - This paper presents a numerical study of particle trapping using quadrupole microfludic dielectrophoretic device. By taking into account the dielectrophoreis, viscous drag, the trajectory of particles flowing through the quadrupole device was obtained. Simulation results show that the device is effective for negative trapping, where particles are effectively trapped at the device centre. The device geometry is optimized by maximizing the dielectrophoretic force.

Key-Words: - Dielectrophoresis, quadrupole, DEP forces, viscous drag, non-dimensional, particle trajetory

1 Introduction

There is increasing interest in developing integrated micro-fluidic systems capable of performing manipulation micro size particles. These integrated micro-systems made of electrical, mechanical and fluidic components have wide applications in areas mentioned above. For example, a micro system can be used in the molecular analysis of cancer cells within a small volume of pathologic fluid to provide cancer prognostic information. A critical necessity for micro-system used to process cell samples is the ability to discriminate and sort cells according to characteristic phenotypes [1-3].

Numerous geometries have been developed to separate particles. The simple case is interdigated electrodes. These devices have been successfully used to in biological fields for separating and manipulating cells [1,3,4]. Cascaded structures are also found applications in manipulation of biological particles [5]. These systems are powerful for 2-D analysis. A few 3-D dielectrophorestic microdevices have also been developed for trapping biological particles [6-8]. A DEP cage was developed by a German team for trapping particles and studying cell properties [7]. Joel proposed a quadrupole structure for trapping of cells [8]. This microelectrode was extended to a ring-dot geometry for trapping of a single cell [9]. The paired-electrode systems [10,11] were developed to successfully herd and transport particles.

This paper is an extension of Joel's work [8] for analysis and development of quadrupole electrode devices. First, the electric field distribution and the DEP forces of this quodrupole device is derived mathematically and the optimum geometry of the quadrupole electrode is achieved. Based on this optimum geometry, the trapping capacity of the device is derived by numerical study of the particle trajectory and motion.

2 Theoretical Background

2.1 Electrical Field Distribution of Quadrupole Electrodes

Suppose the proposed quadrupole electrode is composed of 4 parallel infinite electrical wires. Each wire is charged with either +Q or –Q, as shown in Fig. 1a. As the ratio of wire length to wire diameter is sufficiently large, the structure can be simplified as a 2-D structure for analysis, as shown in Fig. 1b.

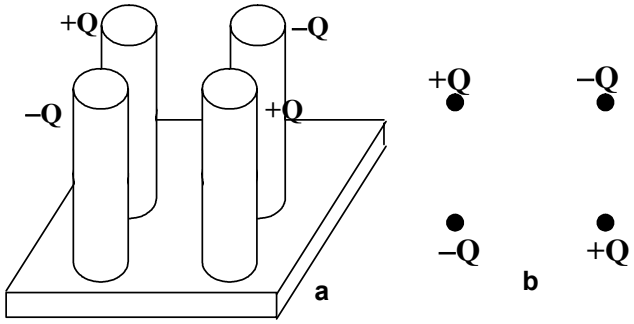

Fig. 1. (a) Schematic of quadrupole electrodes; (b) 2-D structure.

From the electromagnetic theory, a charge element dq at a point M creates an electric field at a point N, which is given by

$$d\vec{E} = \frac{dq}{4\pi\varepsilon_0 r_{MN}^3} i_{MN}\,\vec{r}_{MN} \qquad (1)$$

where $\vec{r}_{MN}$ is the vector from point M to point N, r_{MN} is the magnitude of the vector, ε_0 is the vacuum permittivity.

The electric field strength is obtained by integrating equation 1 along the charge wire

$$\vec{E} = \int \frac{dq}{4\pi\varepsilon_0 r_{MN}^3} i_{MN} \vec{r}_{MN} \qquad (2)$$

For simplicity, the electric field created by a single wire with infinite length is considered and shown in Fig. 2. Suppose the electrical charge density is λ, then $dq = \lambda dl$. As the wire is infinite and symmetric along *r* axis, two mirror charges dq_1 and dq_2 only create a electric field along the r direction

$$dE_r = \frac{\lambda dz}{4\pi\varepsilon\left(z^2 + r^2\right)} \cos\theta = \frac{\lambda r dz}{4\pi\varepsilon\left(z^2 + r^2\right)^{3/2}} \qquad (3)$$

The electric field is obtained

$$E_r = \frac{\lambda r}{4\pi\varepsilon} \int_{-\infty}^{\infty} \frac{dz}{\left(z^2 + r^2\right)^{3/2}} = \frac{\lambda}{2\pi\varepsilon r} \qquad (4)$$

The potential difference between two points P_1 and P_2 is

$$V(r_{P2}) - V(r_{P1}) = -\int_{r_{P1}}^{r_{P2}} E \cdot dl = -\frac{\lambda}{2\pi\varepsilon} \ln \frac{r_{P2}}{r_{P1}} \qquad (5)$$

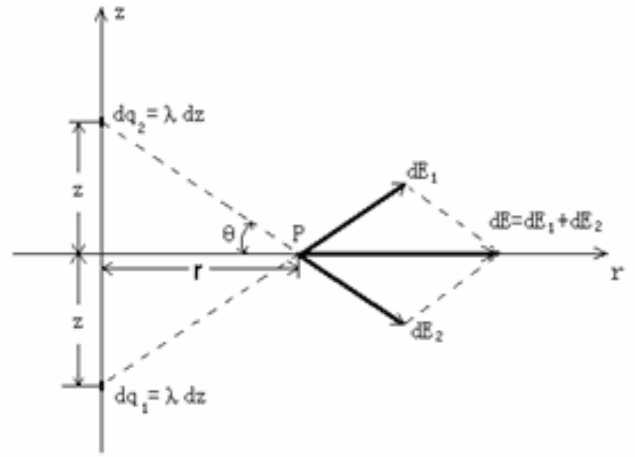

Fig. 2. Electric field distribution of an infinite charge wire.

Suppose the electric charge distributions of these four electrodes are ±λ and their coordinates are $(\pm a, \pm b)$ respectively, as shown in Fig. 3. The potentional distribution at a point (*x*, *y*) is calculated by

$$V(x,y) = \qquad (6)$$
$$-\frac{\lambda}{2\pi\varepsilon} \ln \frac{[(x-a)^2 + (y-b)^2][(x+a)^2 + (y+b)^2]}{[(x-a)^2 + (y+b)^2][(x+a)^2 + (y-b)^2]}$$

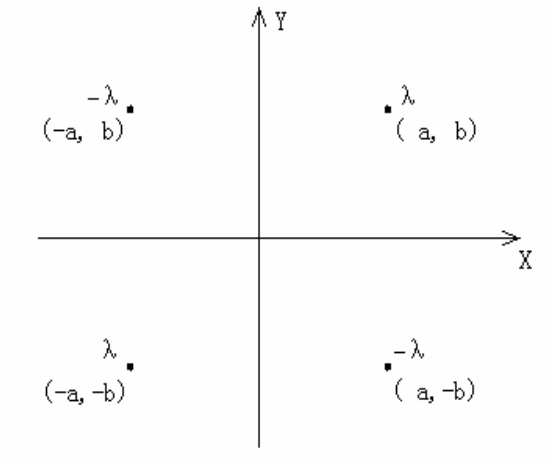

Fig. 3. Electric charge distribution and coordinates of quadrupole electrodes.

The potential distribution is obtained by solving equation 6, as shown in Fig. 4. Obviously, the potential has 4 peak values, which are at the electrode positions.

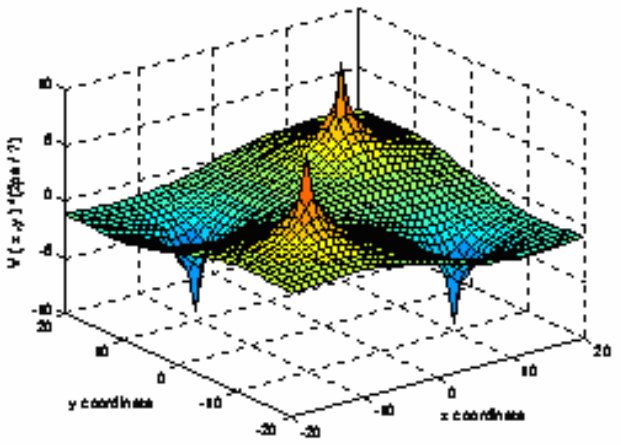

Fig. 4. Potential distribution.

The electrical field is obtained by differentiating equation 6, which gives

$$\vec{E}(x,y) = \frac{\lambda}{2\pi\varepsilon} \left\{ \frac{(x-a)\hat{i} + (y-b)\hat{j}}{(x-a)^2 + (y-b)^2} - \frac{(x-a)\hat{i} + (y+b)\hat{j}}{(x-a)^2 + (y+b)^2} \right.$$
$$\left. + \frac{(x+a)\hat{i} + (y+b)\hat{j}}{(x+a)^2 + (y+b)^2} - \frac{(x+a)\hat{i} + (y-b)\hat{j}}{(x+a)^2 + (y-b)^2} \right\} \qquad (7)$$

where $\hat{i}$ and $\hat{j}$ are unit vectors in x and y directions. The mesh plot of the electrical field distribution is shown in Fig. 5. The electric fields near electrodes is higher than other areas. The minimum electric field is in the centre of the device.

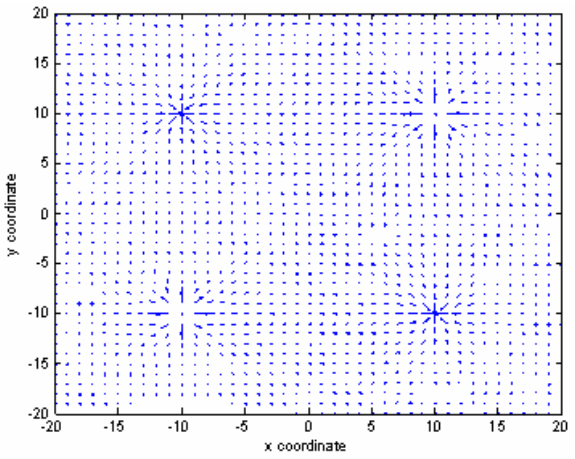

Fig. 5. Electric field distribution.

2.2 DEP forces

Assume a particle is the proposed quadrupole device, the general DEP force is given by

$$\vec{F}_{DEP}(\vec{r}) = 2\pi\varepsilon_0\varepsilon_m R^3 \frac{\varepsilon_p - \varepsilon_m}{\varepsilon_p + 2\varepsilon_m} \nabla \left|\vec{E}(\vec{r})\right|^2 \tag{8}$$

where $\varepsilon_0 = 8.854\times10^{-12}\,Fm^{-1}$ is the permittivity of free space, ε_p and ε_m are relative permittivities of particle and the surrounding medium, R is the particle radius.

Both x and y components of the DEP force are expressed as

$$\begin{aligned}\left(F_{DEP}\right)_x &= 2\pi\varepsilon_m R^3 \frac{\varepsilon_p - \varepsilon_m}{\varepsilon_p + 2\varepsilon_m} \frac{\partial}{\partial x}[E_x^2 + E_y^2] \\ &= 4\pi\varepsilon_m R^3 \frac{\varepsilon_p - \varepsilon_m}{\varepsilon_p + 2\varepsilon_m}[E_x E_{x,x} + E_y E_{y,x}]\end{aligned} \tag{3}$$

$$\begin{aligned}\left(F_{DEP}\right)_y &= 2\pi\varepsilon_m R^3 \frac{\varepsilon_p - \varepsilon_m}{\varepsilon_p + 2\varepsilon_m} \frac{\partial}{\partial y}[E_x^2 + E_y^2] \\ &= 4\pi\varepsilon_m R^3 \frac{\varepsilon_p - \varepsilon_m}{\varepsilon_p + 2\varepsilon_m}[E_x E_{x,y} + E_y E_{y,y}]\end{aligned} \tag{4}$$

where $E_{x,}$, E_y are x and y components of the electric field, and $E_{x,,x}$, $E_{x,,y}$, $E_{y,,x}$, $E_{y,,y}$ are gradients of electric field components. All these formulas are listed in Appendix 1.

2.3 Special case

For simplicity, this part deals with a case near the x axis, i.e., $y = 0$ or $y << b$. From equation (A.1), the x component of the electric field is zero, or $E_x = 0$. So the x component of DEP force in equation 3 can be simplified as

$$\begin{aligned}\left(F_{DEP}\right)_x &= 64\frac{\varepsilon_p - \varepsilon_m}{\varepsilon_p + 2\varepsilon_m}\frac{\lambda^2}{\pi\varepsilon_m} R^3 \times \\ &\frac{a^2 b^2 x[-3x^4 + 2a^2x^2 - 2b^2x^2 + (a^2+b^2)^2]}{[(x-a)^2 + 2(x^2+a^2)b^2 + b^4]^3}\end{aligned} \tag{5}$$

For the sake of analysis, two non-dimensional parameters, β and X, are introduced

$$\beta = \frac{b}{a} \qquad X = \frac{x}{a} \tag{6}$$

where the parameter β is defined as the ratio of device width versus the length, and the X is defined as the ratio of x component position versus the device length. The value X<1 means the area inside the trapping device while X>1 is the area outside of the trapping device.

The DEP force is rewritten as using two parameters β and X

$$\begin{aligned}\left(F_{DEP}\right)_x &= \frac{64}{\pi\varepsilon_m}\frac{\varepsilon_p - \varepsilon_m}{\varepsilon_p + 2\varepsilon_m}\lambda^2\left(\frac{R}{a}\right)^3 \times \\ &\frac{X\beta^2[-3X^4 + 2X^2 - 2\beta^2X^2 + (1+\beta^2)^2]}{[(X^2-1)^2 + 2(X^2+1)\beta^2 + \beta^4]^3} \\ &= k \cdot \frac{X\beta^2[-3X^4 + 2X^2 - 2\beta^2X^2 + (1+\beta^2)^2]}{[(X^2-1)^2 + 2(X^2+1)\beta^2 + \beta^4]^3}\end{aligned} \tag{7}$$

$$\text{where } k = \frac{64}{\pi\varepsilon_m}\frac{\varepsilon_p - \varepsilon_m}{\varepsilon_p + 2\varepsilon_m}\lambda^2\left(\frac{R}{a}\right)^3 \tag{8}$$

Besides physical parameters of particles and medium, equation 7 shows the DEP force also depends on trapping device geometry and particle position, which are represented by β and X respectively. Ideally, the stable particle trapping position should meet with the condition that the DEP force is zero, i.e., $(F_{DEP})_x = 0$. Solving equation 5 by letting it equal to zero, three roots are obtained.

a) Root 1: β = 0
b) Root 2: X = 0
c) Root 3: $X = \pm\sqrt{\dfrac{1-\beta^2+2\sqrt{1+\beta^2+\beta^4}}{3}}$ (9)

Obviously, root 1 is meaningless as the device has 4 electrodes. Root 2 corresponds to the position at the centre of the trapping device. Root 3 is a function of β, or the device geometry.

2.3.1 Trapping position analysis

For a simple case, the value β is chosen 1 to address the effect of particle position on the DEP force. Substitute β =1 into equation 9, the zero DEP force position is calculated as $X = \pm\sqrt[4]{4/3} = \pm1.0746$. This means that zero DEP force is outside of the trapping device. Therefore, the quadrupole device has 3 zero

DEP force positions, one is at the device centre, and the other two are at outside of the device. These trapping positions may be controlled by the sign of k as shown in equation 8. If k <0 or, $\varepsilon_p < \varepsilon_m$, the particles will be trapped at the centre position of X = 0. This can be regarded as a negative trapping. On the other hand, if k >0, or $\varepsilon_p > \varepsilon_m$, the particles will be trapped at the outsides of the device, which corresponds to the positive trapping. The negative trapping will be detailed in the following section.

2.3.2 Negative Trapping

The above analysis shows that the negative trapping is at the vicinity of the device centre. By letting X=0, equation 7 is simplified as

$$\left(F_{DEP}\right)_x = k\frac{\beta^2}{\left(1+\beta^2\right)^4}X \equiv k\,f(\beta)X \qquad (10)$$

where $f(\beta) = \dfrac{\beta^2}{\left(1+\beta^2\right)^4}$ (11)

For the negative trapping, where k is negative in equation 10, the particles will be oscillating at the device centre (X = 0) if there is no resistant force. Generally, the oscillating period varies with the product of k and f(β). The higher the value, the smaller the oscillating period. Thus, if all the other parameters are known, this device could be used as a sensor to detect the permeability of particle or medium.

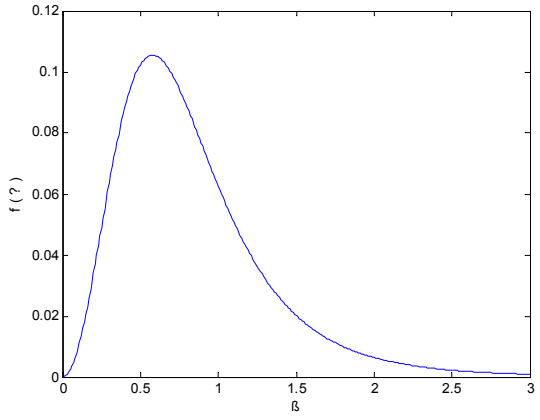

Fig. 6. The plot of f(β) vs. β.

The value of f(β) against β is plotted and shown in Fig. 6. The maximum value of f(β) is obtained by solving the differentiating equation $\dfrac{df(\beta)}{d\beta} = 0$. The maximum value is $\dfrac{27}{256}$ when $\beta = \dfrac{1}{\sqrt{3}}$. This means when the ratio $\dfrac{b}{a} = \dfrac{1}{\sqrt{3}}$, the particle is subjected to the maximum force. This force versus a square quadratic device is given by

$$f(1/\sqrt{3})/f(1) = \frac{27}{16} = 1.6875 \qquad (12)$$

So compared with a square trapping device, the proposed optimum device can increase the trapping force around 70%.

3 Particle Trajectory

3.1 Particle trajectory at x-axis

As the particle is subjected to nonlinear DEP forces, it is difficult to get analytical solution. This paper developed a numerical method to find the trajectory of particle locations. Assume the particle is subjected to a damping force which is proportional to the particle velocity. The following equations are used to calculate particle displacement and velocity.

$$\begin{aligned} V(i+1) &= V(i) + F(N)\Delta t - \mu(V(i) - V(0)) \\ X(i+1) &= X(i) + V(i)\Delta t + F(N)\Delta t^2 - \mu(V(i) - V(0))\Delta t \\ N &= g(X(i+1)) \end{aligned} \qquad (13)$$

where i is the iterative times, N is the particle location, $F(N)$ is the DEP force at the location N, and $g(X(i))$ is the function corresponding to the location $X(i)$.

As discussed in above section, the negative trapping region is located at the device centre region of $-1.0746 < X < 1.0746$; while the positive trapping region is outside of the trapping device of $-\infty < X < -1.0746$ or $1.0746 < X < \infty$. Therefore, if the particle is initially stationery, the particles will be trapped at the centre point, while the particles outside of the centre devices will be pushed away from the device. Thus, if the particles are to be trapped, they must enter the trapping area with a certain speed. Too small or too large initial speeds, the particle cannot enter or pass away the trapping areas, which can not be effectively trapped. Fig. 7 shows the particle trajectory of a few particles with different initial positions; the velocities of these particle are assumed to be zeros. The simulation results indicated that only particles within the trapping area can be effectively trapped at the centre position. However, those particle that are initially at outside of the trapping area are pushed away from the trapping area and cannot be effectively trapped with this device.

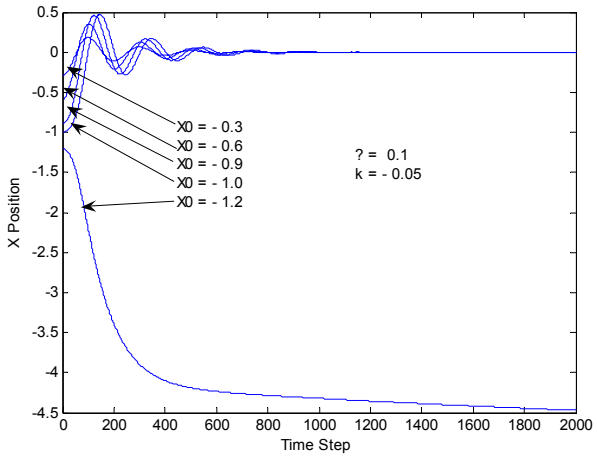

Fig. 7. Particle trajectory with different initial positions.

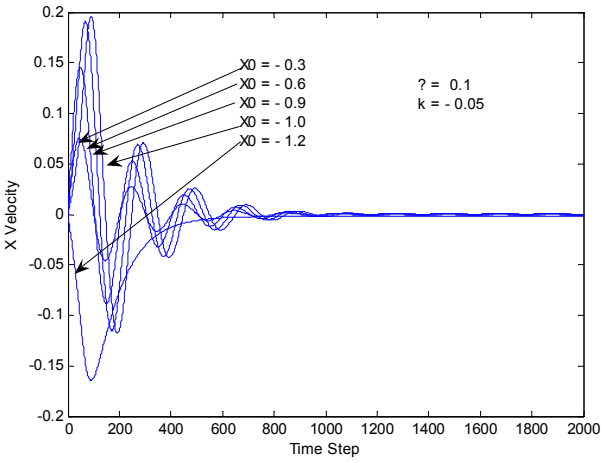

Fig. 8. Velocity of particles with different initial positions.

Velocity profile of these particles at different initial positions is shown in Fig. 8. As can be seen from this figure, the more far from the central position, or the larger X value, the larger velocities of the particles. This is because the particle outside of the trapping area has larger acceleration and has more time to accelerate speed. Except for the particle outside of the trapping area (X = -1.2), the particle oscillating periods have no obvious variance, even though the amplitude varies with initial position.

The effect of particle velocity on the trapping effect is shown in Fig. 9. It can be seen from this figure that the particles only having appreciate initial velocities can be effectively trapped. Those particles with much higher or lower velocities cannot enter the trapping area.

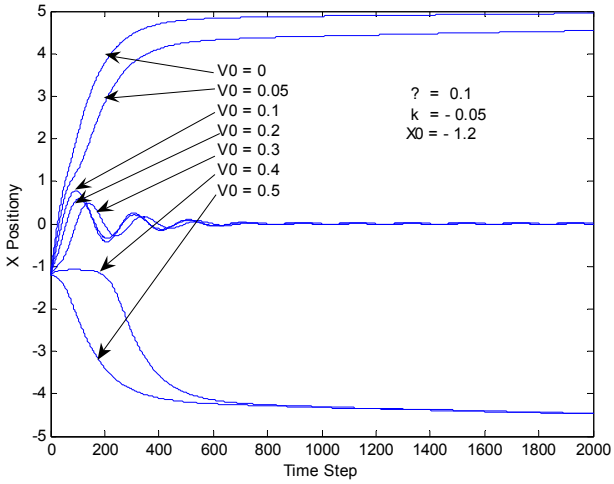

Fig. 9. Particle trajectory at different initial velocities.

Fig. 10 shows the negative and positive trapping. Again, negative k value corresponds to negative trapping while positive *k* value is for positive trapping. Particles for negative trapping is trapped at the device centre while the positive trapping is located outside of the trapping device.

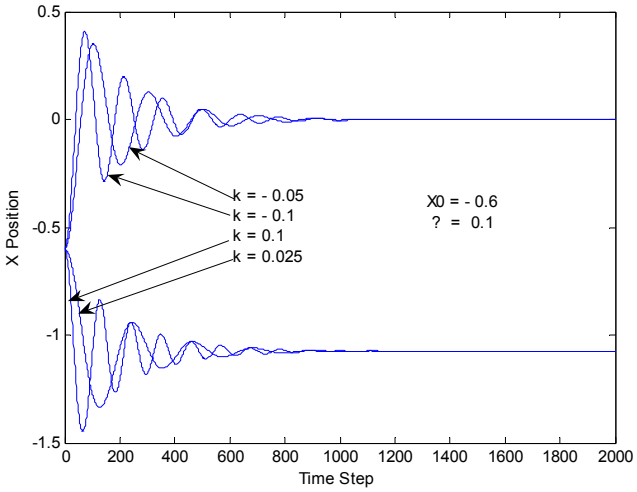

Fig. 10. Negative and positive trapping.

The damping coefficient also plays an important role in trapping particles. Fig. 11 shows particle trajectory at two typical damping conditions, where the particle are projected into the device from initial position outside of the trapping device. It can be seen from this figure the higher damping will reduce the oscillating period and the peak velocity as well.

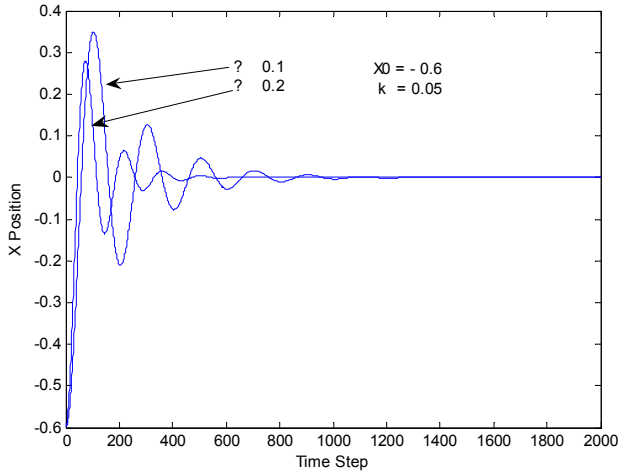

Fig. 11. Particle trajectory at different dampings.

3.2 Particle trajectory at arbitrary position

The particle motion at any arbitrary position will be addressed by 2-D plots. Suppose four particles with same physical properties are projected into the trapping devices from different starting positions, as shown in Fig. 12. Coordinates (X_0, Y_0) represent particle initial positions. The particle trajectory is shown in this figure. As can be seen from this figure, the particle which is close the electrode is pushed away from the trapping centre. Other three particles, far from the electrodes, are effectively trapped in the centre position.

Fig. 13 shows the effect of particle velocity on the trapping effect. Similar to 1-D trapping, the 2-D trapping also shows only appropriate velocity can contribute to effecting trapping. Particle with too large or too small velocities can be trapped in the device.

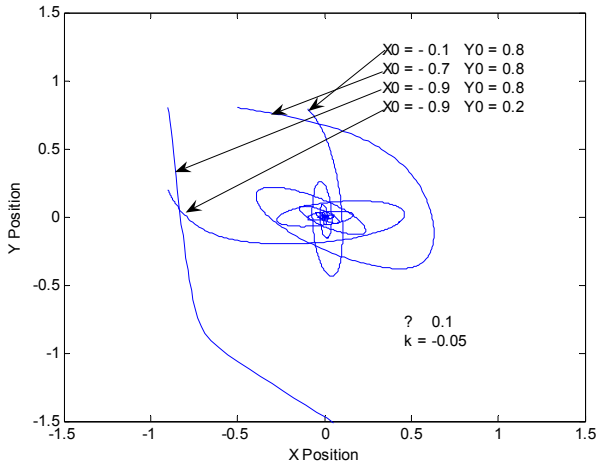

Fig. 12. Trajectory of particles with different initial positions.

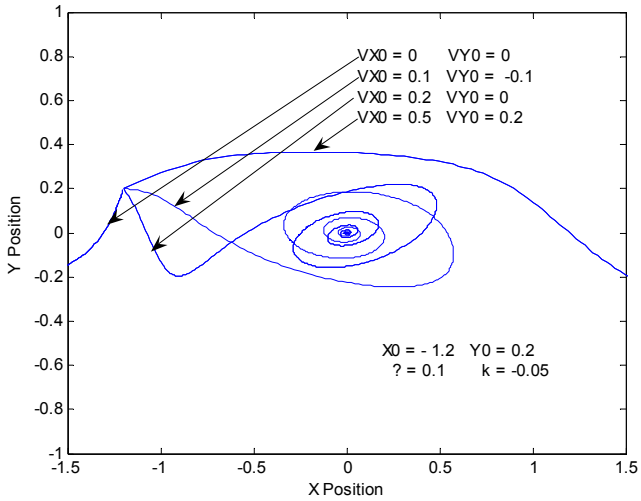

Fig. 13. Trajectory of particles with different initial velocities.

3.3 Device conceptual design

Based on the above analysis, a conceptual design of the proposed quadrupole electrode device is shown in Fig. 14. This is an electrode array comprising of 4 quadrupole electrode elements. The physical parameters for each device are shown in Table 1.

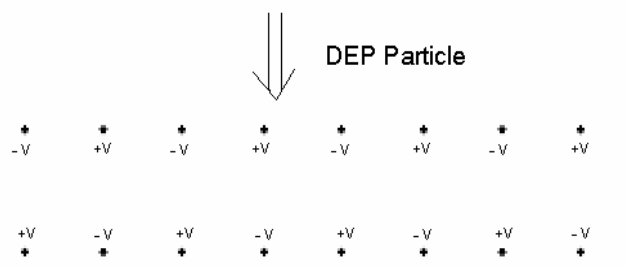

Fig. 14. Quadrupole electrode array.

Table 1. Quadrupole electrode device parameters.

Electrode length	Electrode width	Wire diameter	Wire length
100μm	57.7μm	5μm	60μm

The proposed device will be fabricated and the practical of such device in particle trapping will be evaluated in future.

4 Conclusion

In this paper, a numerical study was presented to investigate trapping of particles using negative DEP based on a quadrupole microfludic device. The device is optimized by maximizing the DEP force. The effects of particle initial position and velocity on the particle trapping stability are addressed. If the

particle is more close to the electrodes, it would be hard to be stably trapped. Using this device, particles only having appropriate velocities, not too large or small, can be effectively trapped. The practical trapping device is conceptually designed.

Acknowledgement
This project is supported by the Australian Research Council through a discovery project.

References:

[1] X.B. Wang, J. Yang, Y. Huang, J. Vykoukal, F.F. Becker, P.R.C. Gascoyne, Cell separation by dielectrophoretic field-flow-fractionation, *Anal. Chem.* 72, 2000, 832-9.

[2] T. Heida, W.L.C. Rutten, E. Marani, Understanding dielectrophoretic trapping of neuronal cells: modeling electric field, electrode-liquid interface and fluid flow, *J. Phys. D: Appl. Phys.* 35, 2002, 1592-602.

[3] H.B. Li, R. Bashir, Dielectrophoretic separation and manipulation of live and heat-treated cells of Listeria onmicrofabricated devices with interdigitated electrodes, *Sensor Actuat. B – Chem.* **86**, 2002, pp. 215-21.

[4] Y. Huang, X.B. Wang, F.F. Becker, P.R.C. Gascoyne, Introducing dielectrophoresis as a new force field-flow fractionation, *Biophys. J.*, 73, 1997, pp. 1118-29.

[5] H. Morgan, M.P. Hughes, N.G. Green, Separationof submicron bioparticles by dielectrophoresis, *Biophys. J.*, 77, 1999, pp. 516-25.

[6] J. Suehiro, R. Pethig, The dielectrophoretic movement and positioning of a biological cell using a three-dimensional grid electrode system *J. Phys. D: Appl. Phys.*, 31, 1998, pp. 3298-305.

[7] T. Schnelle, T. Muller, C. Reichle, G. Fuhr, Combined dielectrophoretic field cages and laser tweezers for electrotation, *Appl. Phys. B*, 70, 2000, pp. 267-74.

[8] T. Voldman, M. Toner, M.L. Gray, M.A. Schmidt, Design and analysis of extruded quadrupolar dielectrophoretic traps, *Journal of Electrostatics*, 57, 2003, pp. 69-90.

[9] B.M. Taff, J. Voldman, A scalable addressable positive-dielectrophoretic cell-sorting array, Anal. Chem., 77, 2005, pp. 7976-83.

[10] S. Fiedler, S.G. Shirley, T. Schnelle, G. Fuhr, Dielectrophoretic sorting of particles and cells in a microsystem, Anal. Chem., 70, 1998, pp. 1909-15.

[11] D.F. Chen, H. Du, W.H. Li, A 3D paired microelectrode array for accumulation and separation of microparticles, *Journal of Micromechanics and Microengineering*, 16 (7), 2006, pp.1162-69.

Appendix 1. Formulas of electric field components and their derivatives.

$$E_x = \frac{\lambda}{2\pi\varepsilon}\{\frac{x-a}{(x-a)^2+(y-b)^2} - \frac{x-a}{(x-a)^2+(y+b)^2} + \frac{x+a}{(x+a)^2+(y+b)^2} - \frac{x+a}{(x+a)^2+(y-b)^2}\} \quad (A.1)$$

$$E_y = \frac{\lambda}{2\pi\varepsilon}\{\frac{y-b}{(x-a)^2+(y-b)^2} - \frac{y+b}{(x-a)^2+(y+b)^2} + \frac{y+b}{(x+a)^2+(y+b)^2} - \frac{y-b}{(x+a)^2+(y-b)^2}\}$$

$$E_{x,x} = \frac{\partial}{\partial x}E_x = \frac{\lambda}{2\pi\varepsilon}\{\frac{(y-b)^2-(x-a)^2}{[(x-a)^2+(y-b)^2]^2} - \frac{(y+b)^2-(x-a)^2}{[(x-a)^2+(y+b)^2]^2} + \frac{(y+b)^2-(x+a)^2}{[(x+a)^2+(y+b)^2]^2} - \frac{(y-b)^2-(x+a)^2}{[(x+a)^2+(y-b)^2]^2}\}$$

$$E_{x,y} = \frac{\partial}{\partial y}E_x = \frac{\lambda}{2\pi\varepsilon}\{\frac{(x-a)^2-(y-b)^2}{[(x-a)^2+(y-b)^2]^2} - \frac{(x-a)^2-(y+b)^2}{[(x-a)^2+(y+b)^2]^2} + \frac{(x+a)^2-(y+b)^2}{[(x+a)^2+(y+b)^2]^2} - \frac{(x+a)^2-(y-b)^2}{[(x+a)^2+(y-b)^2]^2}\}$$

$$E_{y,x} = \frac{\partial}{\partial x}E_y = -\frac{\lambda}{\pi\varepsilon}\{\frac{(x-a)(y-b)}{[(x-a)^2+(y-b)^2]^2} - \frac{(x-a)(y+b)}{[(x-a)^2+(y+b)^2]^2} + \frac{(x+a)(y+b)}{[(x+a)^2+(y+b)^2]^2} - \frac{(x+a)(y-b)}{[(x+a)^2+(y-b)^2]^2}\}$$

$$E_{y,y} = \frac{\partial}{\partial y}E_y = -\frac{\lambda}{\pi\varepsilon}\{\frac{(x-a)(y-b)}{[(x-a)^2+(y-b)^2]^2} - \frac{(x-a)(y+b)}{[(x-a)^2+(y+b)^2]^2} + \frac{(x+a)(y+b)}{[(x+a)^2+(y+b)^2]^2} - \frac{(x+a)(y-b)}{[(x+a)^2+(y-b)^2]^2}\} \quad (A.2)$$